J|A|C|S
ARTICLES

Published on Web 01/20/2009

Gas−Surface Chemical Reactions at High Collision Energies?

Michael J. Gordon,[†] Xiangdong Qin,[‡] Alex Kutana,[‡] and Konstantinos P. Giapis*[,‡]

Department of Chemical Engineering, University of California—Santa Barbara, Santa Barbara, California 93106-5080, and Division of Chemistry and Chemical Engineering, California Institute of Technology, Pasadena, California 91125

Received October 3, 2008; E-mail: giapis@cheme.caltech.edu

Abstract: Most gas−surface chemical reactions occur via reaction of adsorbed species to form a thermal-energy ($\sim kT$) product; however, some instances exist where an energetic projectile directly reacts with an adsorbate in a single-collision event to form a hyperthermal product (with a kinetic energy of a few eV). Here we show for the first time that 30−300 eV F^+ bombardment of fluorinated Ag and Si surfaces produces "ultrafast" F_2^- products with exit energies of up to 90 eV via a multistep direct-reaction mechanism. Experiments conclusively show that the projectile F atom ends up in the fast molecular product despite the fact that the impact energy is far greater than typical bond energies.

Introduction

Gas−surface reactions typically proceed via the Langmuir−Hinshelwood mechanism, where atoms or molecules adsorb onto a surface, diffuse around, and subsequently react to form a product molecule that leaves the surface (desorbs) at thermal energies ($\sim kT$).[1] However, another class of reactions exists where an adsorbate directly reacts with an impinging gas molecule (or energetic projectile) through a collision-based mechanism to form a "fast" product—the so-called Eley−Rideal (ER) mechanism.[2−6] ER products are distinct because they are frequently excited (rotation−vibration) and tend to leave the surface at hyperthermal energies (up to a few eV) in specific directions that correlate with the incoming projectile geometry.[7] Our current understanding of ER reactions, from the perspective of detailed collision dynamics and energy transfer, is largely qualitative. Most observations suggest that a translationally hot product can be generated in two limiting situations: (i) a light atom strikes a heavy adsorbate, becoming trapped in the attractive well of the heavy-atom recoil as it leaves the surface or (ii) a heavy projectile scatters off the surface and abstracts ("scoops up") a lighter atom on the outgoing trajectory path. Therefore, ER products would seem to form in single-collision events only when (i) the partners are mismatched in mass and (ii) the post-collision kinetic energy of each fragment that makes up the product molecule must be less than typical bond energies (otherwise the product molecule would not remain intact as it leaves the surface). As such, ER reactions should not occur at high impact energies. Here, we present experimental evidence and theoretical support for a new class of ER reactions at high impact energies (up to 300 eV) that involve equal-mass partners and multiple collision events and form "ultrafast" products (up to 90 eV) that surprisingly remain intact after leaving the surface.

Specifically, we have used F^+ projectiles (30−300 eV), which undergo ER abstraction of F atoms from fluorinated Ag and Si surfaces, to form F_2^- products with substantial kinetic energies (up to ~90 eV). Energy analysis of F_2^- leaving the surface reveals two distinct exit channels: one low-energy component attributed to sputtering and another higher-energy component that directly correlates with the F^+ incident energy. The fast-F_2^--exit component *only* occurs for F^+ bombardment, indicating that the product must contain the projectile F atom. Molecular dynamics also predicts fast-F_2 formation *at the observed experimental energy* through a direct-collision sequence that results in two F species in close proximity leaving the surface with large, yet comparable, exit velocities.

Experimental evidence for ER mechanisms can take several forms:[2] (i) nonthermal translational energies of products, (ii) product energies that depend on the projectile energy (i.e., momentum memory), (iii) rotationally and/or vibrationally excited products, and (iv) product distributions that depend on impact geometry or peak at off-normal angles. Documented examples of ER mechanisms usually involve projectiles at "low" collision energies accessible by molecular-beam methods.[8] Notable examples include D- and Cl-atom abstraction by H atoms from D/Cu(111),[9] Cl/Au(111),[10] and D/Si(100)[11] as well as proton "pickup" from Pt(111) by $N(C_2H_4)_3N$.[12] Other studies with low-energy ion beams (<50 eV) have demonstrated direct abstraction of protons from pyridine-covered Ag(111) (pyridine

[†] University of California—Santa Barbara.
[‡] California Institute of Technology.

(1) Weinberg, W. H. *Dynamics of Gas−Surface Interactions*; Rettner, C. T., Ashford, M. N. R., Eds.; Royal Society of Chemistry: London, 1991.
(2) Maazouz, M.; Barstis, T. L. O.; Maazouz, P. L.; Jacobs, D. C. *Phys. Rev. Lett.* **2000**, *84*, 1331.
(3) Kratzer, P. *J. Chem. Phys.* **1997**, *106*, 6752.
(4) Dinger, A.; Lutterloh, C.; Kuppers, J. *Chem. Phys. Lett.* **1999**, *311*, 202.
(5) Kim, J. Y.; Lee, J. *Phys. Rev. Lett.* **1999**, *82*, 1325.
(6) Yi, S. I.; Weinberg, W. H. *Surf. Sci.* **1998**, *415*, 274.
(7) Rettner, C. T.; Auerbach, D. J. *Science* **1994**, *263*, 365.
(8) Rettner, C. T.; Auerbach, D. J.; Tully, J. C.; Kleyn, A. W. *J. Phys. Chem.* **1996**, *100*, 13021.
(9) Rettner, C. T.; Auerbach, D. J.; Lee, J. *J. Chem. Phys.* **1996**, *105*, 10115.
(10) Rettner, C. T. *J. Chem. Phys.* **1994**, *101*, 1529.
(11) Buntin, S. A. *J. Chem. Phys.* **1998**, *108*, 1601.
(12) Kuipers, E. W.; Vardi, A.; Danon, A.; Amirav, A. *Phys. Rev. Lett.* **1991**, *66*, 116.

projectiles);[13,14] H, F, CH_3, and C_2H_3 groups from self-assembled monolayers by pyrazine and pyrene;[15] O from Ag(111) by NO^+,[2] and CO and CO_2 from Pt(111) by Cs^+.[16] Energetic O^+ (10−60 eV) has also been shown to remove O atoms from oxidized Si to form fast O_2^- (∼8 eV).[17] In all of these cases, product energies are comparable to or a few times greater than the bond energy; this situation is understandable because the relative kinetic energy of the fragments that make up the final molecule cannot be greater than typical bond energies. In fact, a single collision event, when it occurs at high energy, can never result in a scattered projectile and recoil with small relative kinetic energies (i.e., relative to the center-of-mass of the product molecule). To date, no ER mechanisms that result in highly energetic products (>10 eV) have been observed. The reason may be found in the collision cascade: when the collision energy is raised, gas−surface reactions transition into hard-sphere scattering processes in which the projectile cascade sputters atoms and clusters from the surface.[18] At such energies, chemical "reactions" per se become secondary compared to momentum-driven sputtering processes; direct reactions (even if they occur through multiple collisions) are simply washed out. However, we show here that direct reactions do occur at high impact energies, yielding highly energetic (10−100 eV) products; furthermore, these experiments suggest that ultrafast products should be formed in many other collision systems.

Experimental Section

Scattering experiments were conducted in a custom-built, low-energy ion scattering system that has been described elsewhere.[19] Briefly, the system utilizes an inductively coupled plasma (ICP)-source, high-voltage beamline (20 keV) with a 60° magnetic mass filter and deceleration optics to deliver high fluxes of isotopically pure species at low energies (20−1500 ± 2 eV fwhm) onto a grounded target under UHV conditions. The ion-beam energy and spatial profile were characterized with a 180° electrostatic sector and 2D wire sensor at the target position. For F^+ and $^{22}Ne^+$ beams, the ICP was run at 2 mTorr/600 W with pure Ne or CF_4/O_2 mixes. Scattered species were analyzed with a triply differentially pumped detector system with an electrostatic sector and quadrupole mass filter to measure the energy distribution and charge state of each species leaving the target. Experiments were conducted at a laboratory angle $\theta_L = 90°$ in specular reflection with beam currents in the 1−10 μA range over 2 mm. Product spectra were recorded under steady-state scattering conditions at room temperature; all of the samples were sputter-cleaned with 5 keV Ar^+, and the target surface could be flooded with XeF_2 gas through a doser pipe situated ∼1 cm from the surface.

Results and Discussion

Typical spectra for F^- and F_2^- leaving an Ag surface under F^+ bombardment at various projectile energies ($E_0 = 30-175$ eV) are shown in Figure 1a,b, respectively. Intensities were normalized by beam current and scattering cross section (F^- data only) for an F + Ag collision at $\theta_L = 90°$ using the

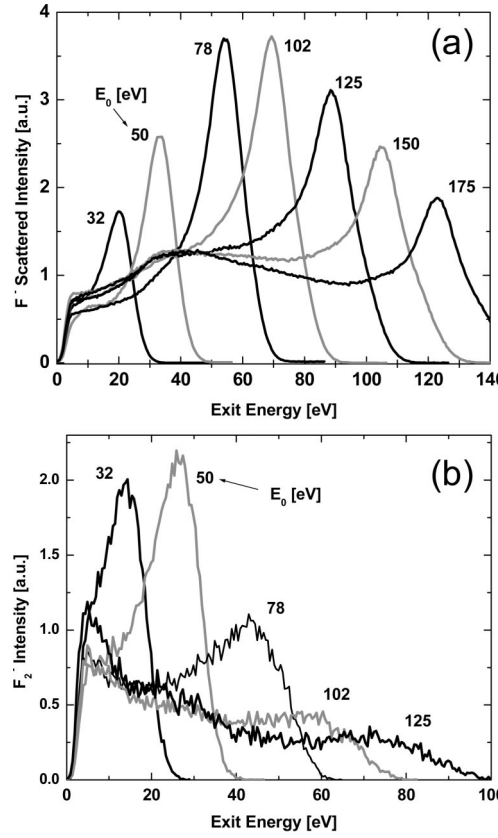

Figure 1. Energy distributions of (a) F^- and (b) F_2^- leaving the surface when Ag is bombarded with F^+ projectiles at various energies (shown as E_0) for $\theta_L = 90°$.

Thomas−Fermi−Molière (TFM) potential.[20,21] Several trends in the data are worth noting: (i) F_2^- is produced, (ii) two distinct peaks can be seen for both F^- and F_2^-, (iii) the low-energy peak (∼10 eV) for each ion appears to be invariant with projectile energy (reminiscent of cascade sputtering[18]), and (iv) the high-energy F^- and F_2^- peaks shift upward as the impact energy is increased. The charge-exchange picture of F scattering in this case is efficient Auger or resonant neutralization of the projectile on the incoming path and hard collision (which may lead to F*, F^+, or F^-) followed by electron capture (or detachment) on the outgoing path. Copious F^- is not unexpected because the anion level of F shifts[22] well below the Fermi level of the target as a result of image-charge effects when $R_{min} < 4$ Å. The intensity of negative ions leaving the target surface (relative to that of F^+) was quite large (>2−3 orders of magnitude) for all impact energies. In general, the F^- yield (total negative ions) goes through a maximum. This behavior is due to perpendicular velocity effects[23] at low E_{exit} (i.e., more anions survive because of shorter contact time on the outgoing path) and cross-section/subplantation[24] effects at higher E_0 (i.e., the projectile preferentially scatters forward and/or penetrates deeper into the target, so the 90° flux is lower).

(13) Wu, Q.; Hanley, L. *J. Phys. Chem.* **1993**, *97*, 8021.
(14) Wu, Q.; Hanley, L. *J. Phys. Chem.* **1993**, *97*, 2677.
(15) Morris, M. R.; Riederer, D. E.; Winger, B. E.; Cooks, R. G.; Ast, T.; Chidsey, C. E. D. *Int. J. Mass Spectrom. Ion Processes* **1992**, *122*, 181.
(16) Kim, J. H.; Lahaye, R. J. W. E.; Kang, H. *Surf. Sci.* **2007**, *601*, 434.
(17) Quinteros, C. L.; Tzvetkov, T.; Jacobs, D. C. *J. Chem. Phys.* **2000**, *113*, 5119.
(18) Sigmund, P. *Phys. Rev.* **1969**, *184*, 383. Thompson, M. W. *Phil. Mag.* **1968**, *18*, 377.
(19) Gordon, M. J.; Giapis, K. P. *Rev. Sci. Instrum.* **2005**, *76*, 083302.
(20) Gordon, M. J.; Mace, J.; Giapis, K. P. *Phys. Rev. A* **2005**, *72*, 012904.
(21) Mace, J.; Gordon, M. J.; Giapis, K. P. *Phys. Rev. Lett.* **2006**, *97*, 257603.
(22) Ustaze, S.; Guillemot, L.; Esaulov, V. A.; Nordlander, P.; Langreth, D. C. *Surf. Sci.* **1998**, *415*, L1027.
(23) Maazouz, M.; Guillemot, L.; Esaulov, V. A. *Phys. Rev. B* **1997**, *56*, 9267.
(24) Rabalais, J. W. *Principles and Applications of Ion Scattering Spectrometry: Surface Chemical and Structural Analysis*; John Wiley and Sons: Hoboken, NJ, 2003.

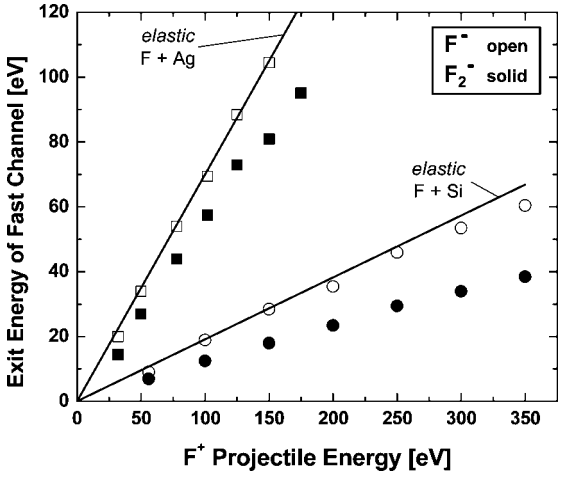

Figure 2. Exit energies of fast F^- and F_2^- off Ag and Si along with binary elastic predictions for F + Ag and F + Si at $\theta_L = 90°$.

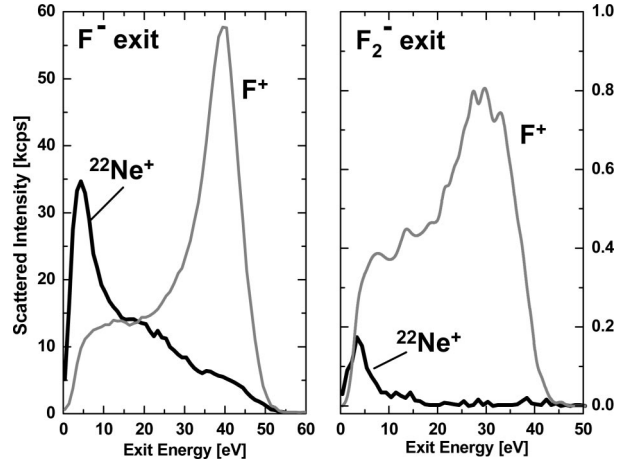

Figure 3. F^- and F_2^- product energy distribution functions for F^+ and $^{22}Ne^+$ projectiles when an Ag surface is flooded with thermal XeF_2.

Although yield data are informative, energy distributions of species leaving the target are more useful in determining the actual scattering mechanism. For instance, both F^- and F_2^- leaving the surface have well-defined, high-energy peaks that appear to scale with the incoming projectile energy. These peak locations are summarized in Figure 2, along with the elastic prediction[20,21] for a single-scatter F + Ag or F + Si collision giving a 90° exit. As shown, the fast-F^- exit is in excellent agreement with elastic binary collision theory; similar results for F^+ exits off the same surfaces have been shown previously.[21]

However, the most notable feature in the data is the *highly nonthermal* F_2^-, which is suggestive of a direct (ER) mechanism. This peak could originate from (i) "sputtering" of F_2 off the surface by the projectile cascade or (ii) ER-like abstraction (i.e., the projectile F atom ends up in the fast-F_2^- exit via direct or scattering-mediated abstraction of a surface-bound F). Process (i) can be eliminated on several grounds. The high exit energy (≫surface binding energy), the shift in the distribution maximum with E_0, and the lack of a high-energy tail are all contrary to standard sputtering theories and experiment.[18] Thus, it seems that direct reaction [process (ii)] could be responsible for the fast F_2^-. To test this hypothesis further, the target was flooded with XeF_2 gas from a doser pipe during F^+ or $^{22}Ne^+$ bombardment. In these experiments, the scattering chamber pressure was increased from $<10^{-9}$ to 7×10^{-7} Torr by leaking in XeF_2 to saturate the target surface with fluorine. We specifically chose $^{22}Ne^+$ projectiles instead of $^{20}Ne^+$ to remove all possibilities of $^{20}Ne^+$ contamination in the F^+ beam or "false counting" of mass 20 when the quadrupole in the scattered-product detector was set to mass 19.

Figure 3 summarizes typical ion-energy distribution functions for the XeF_2 dosing experiments for a 60 eV projectile. It can be clearly seen that fast F_2^- is absent for the $^{22}Ne^+$ projectile case. The data also show that (i) F^+ and $^{22}Ne^+$ generate similar amounts of low-energy sputtered F^- when the surface is fluorinated, (ii) more low-energy F^- is generated when the surface is flooded with thermal F (i.e., XeF_2 dosing) than for F^+ projectiles alone, and (iii) small amounts of F_2^- at low energy (3−5 eV) are sputtered from the surface by $^{22}Ne^+$. All of these trends make sense with respect to increased sputtering due to higher surface fluorination, sputtering that is projectile-insensitive (only momentum is at play), and production of fast F_2^- via an ER mechanism. This experiment eliminates the possibility of scattering-mediated abstraction,[17] where the incoming projectile creates an F recoil that directly "scoops up" another F on the outgoing path. Such a mechanism should be operable for both F^+ and $^{22}Ne^+$ projectiles; however, this is not seen. By the process of elimination, it appears that fast F_2^- is formed through an ER-type direct reaction where the projectile F atom ends up in the F_2^- exit.

Additional support for a direct mechanism comes from molecular dynamics (MD) simulations.[25] Figure 4a shows a trajectory "history" that generates a fast, vibrationally excited F_2 exit when F hits a fluorinated Ag surface at 50 eV. Fast F_2 is made via five steps: (i) projectile **P** (black) hits F atom **A**, after which **P** forward-scatters and **A** recoils (red); (ii) **P** collides hard with an Ag atom and scatters at ∼95−100°; (iii) **P** nudges the moving F atom **A** again; (iv) ***P*** deflects off another F, leaving the surface; and (v) the moving F atom **A** nudges another surface F atom **B** and leaves with a velocity vector similar to that of **P**. The two exiting F atoms combine and leave the surface in a vibrationally hot state (the trajectory oscillation should be noted: further timesteps clearly show the F_2 vibration). This collision sequence is clearly direct (Eley−Rideal), retains a considerable portion of the projectile momentum (i.e., **P** hits its final partner two times), and the resulting F_2 molecule contains the projectile F atom. The role of the surface in this case is to act as a kinematic mediator that enables the fast-F_2 channel by preparing the trajectory and energy of the projectile and its final partner. For the case shown (and similar direct sequences), the F_2 final energy falls in the 24−28 eV range for a 50 eV projectile.

When all of the MD trajectories resulting in F_2 are binned according to the final F_2 energy (Figure 4b), a large peak near 26 eV is seen, exactly matching that measured in our experiments. The fast-F_2 peak width difference between the experimental and MD results is easily explained by the finite-energy width of the F^+ projectile beam in the experiment (50 ± 2 eV

(25) MD was carried out using a superposition of modified Morse−Molière potentials for F + F and F + Ag. At each E_0, 10^7 primaries were launched at the F-on-Ag target [one F and two Ag(111) layers] with 45° incidence versus the surface normal, random impact parameter, and random azimuth. The cascade was followed until all species had kinetic energies of <10 eV. An "intact" F_2 was defined as $E_{tot}^{F_2} = K_{tot}^{F_2} + U_{tot}^{F_2} < 0$, where $K_{tot}^{F_2}$ is the kinetic energy of F_2 in the center-of-mass system and $U_{tot}^{F_2}$ is the potential energy. Total energies for F and F_2 from density-functional theory (DFT) calculations were −99.7208 and −199.4968 hartree, respectively; the optimized bond length for F_2 was found to be 2.6549 bohr. See the Supporting Information for details.

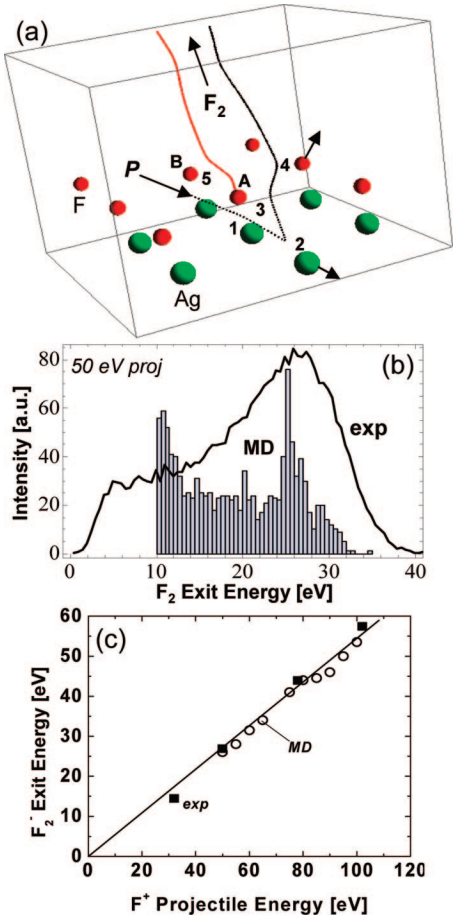

Figure 4. Fast F_2 formation. (a) MD trajectory history for a 50 eV F projectile (**P**; black line) reacting directly with a fluorinated Ag surface to generate F_2 at a high exit energy (27 eV). See the text for the collision sequence. (b) Experimental F_2^- exit energy (solid) and MD (histogram) results for F_2 leaving the surface for 50 eV incident F (see ref 25). (c) Fast-F_2^- peak location for various F^+ impact energies on fluorinated Ag: (solid) experimental and (open) MD results. The solid line is to guide the eye only.

fwhm). Differences at low F_2 exit energies are related to electron detachment from F_2^- at low exit velocities, i.e., a slow F_2^- leaving the surface easily loses its electron back to the surface and is not seen in the experiment (i.e., perpendicular velocity effects). As added evidence, the fast F_2 peak from MD calculations was tallied for different impact energies; Figure 4c demonstrates that this "direct" collision sequence from MD agrees extremely well with experiment. We should mention that a scattering-mediated abstraction reaction (i.e., projectile F hits a surface F, which then "scoops up" another F on the exit) was found via MD; however, this collision sequence was eliminated given that the negative control experiment with $^{22}Ne^+$ and XeF_2 on Ag (see Figure 3) did not give fast F_2^-.

Finally, it is worth commenting on the intensity of scattered F_2^- as a function of F^+ impact energy. The decreasing F_2^- yield at high E_0 results from increased vibrational excitation of ER-created F_2^-, leading to autodetachment[17] (in which case the F_2 neutral would not be seen), or complete dissociation of vibrationally hot $F_2^{0/-}$. The MD results for fast exits consistently

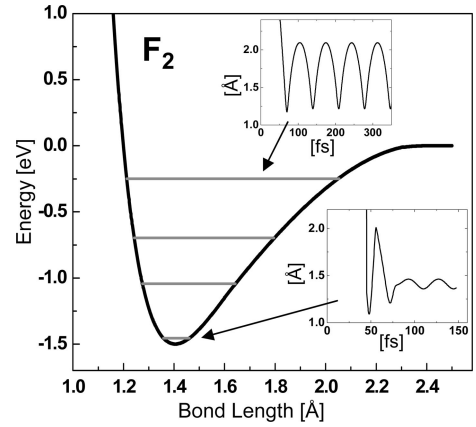

Figure 5. Vibrational excitation of fast F_2 leaving a fluorinated Ag surface for 50 eV F^+ impact, as determined from MD. The potential energy curve and associated vibrational levels (classical) of four different exits are shown. The insets show the F_2 bond length vs time for two specific fast-F_2 exits.

show rotation and vibration in the F_2 product. For instance, Figure 5 gives a summary of the results for four vibrationally excited fast F_2 molecules leaving the surface for 50 eV F impact as a result of direct reactions similar to that shown in Figure 4a. The insets show the F−F bond length of the final F_2 product as a function of the collision time; short times (<50−100 fs), where the bond length is physically impossible (>2.1−2.2 Å), are associated with the projectile approach to the surface and "pre-molecule-formation" collisions (see Figure 4a). These classical trajectory calculations predict a wide range of vibrational excitation in the F_2 product, all the way up to the dissociation limit. In addition, the anharmonicity in the potential energy curve near the dissociation threshold becomes apparent in the temporal variation of the F−F bond length (Figure 5, upper inset). Although the potential energy curve changes when the F_2 becomes an anion, it is highly probable that the fast F_2^- product is vibrationally excited.

Conclusion

In summary, we have shown that Eley−Rideal abstraction involving F^+ projectiles and fluorinated Ag and Si surfaces can occur at high impact energies (30−300 eV), resulting in hyperthermal F_2^- ions leaving the surface at energies of tens of electron volts. Energy analysis of the F_2^- products as well as bombardment of externally fluorinated surfaces with $^{22}Ne^+$ rather than F^+ shows that F^+ projectiles are required for fast-F_2^- formation. MD results also show that a direct-reaction sequence involving multiple collisions can form an F_2 product with a high translational energy that correlates exactly with experiment.

Acknowledgment. This study was based on work supported by the National Science Foundation under Grant CTS-0613981. Applied Materials, Inc. donated equipment essential for the experiments.

Supporting Information Available: Details of MD and DFT calculations. This material is available free of charge via the Internet at http://pubs.acs.org.

JA807672N